Studies of Oxygen Species in Synthetic Todorokite-like Manganese Oxide Octahedral Molecular Sieves

Yuan-Gen Yin,[†] Wen-Qing Xu,[†] Yan-Fei Shen,[†] and Steven, L. Suib*[,†,‡,§]

Department of Chemistry, Department of Chemical Engineering, and Institute of Materials Science, University of Connecticut, Storrs, Connecticut 06269-3060

C. L. O'Young*

Texaco Research Center, Texaco, Inc., P.O. Box 509, New York 12508

Received April 5, 1994. Revised Manuscript Received June 20, 1994[⊗]

Manganese oxide octahedral molecular sieves of 3 × 3 tunnel structure (OMS-1) doped with various cations possess high thermal stability and were studied by means of temperature-programmed desorption and reduction by H_2 and CO. Different oxygen species can be discerned according to their peak positions in the temperature-programmed desorption and reduction and assigned to chemisorbed dioxygen, oxygen atoms bound to Mn^{2+}, and those bound to Mn^{4+} ions in the framework. Differences in peak positions and availabilities of these species during TPD and TPR an be explained by creation of nascent Mn^{2+} ions during TPR. The effects of doping cations on the reactivity and availability of these oxygen species are demonstrated to be more pronounced in TPR in H_2 or CO than in TPD. In some instances, the trends of changes in reactivity and availability of the oxygen species due to doping of Cu^{2+}, Ni^{2+}, Zn^{2+}, and Mg^{2+} correlated with the changes in the heat of formation of oxides of these cations. Temperature-programmed reactions with methane show some reactivity of these doped OMS-1 materials. Pulse reactions with CO show higher reactivity of Cu-doped OM-1 than with butane. However, the recovery of Cu-doped OMS-1 by reoxidation with oxygen pulses seems rather incomplete at the same temperature.

Introduction

Manganese oxides, especially β-MnO_2 (pyrolusite), have long been used as a major constituent of catalysts.[1-3] Manganese oxides also find important applications as electrochemical materials[4,5] and in manufacturing SYNROC (synthetic rock, i.e., hollandite) for storage of radioactive wastes.[6] Interest in adsorptive and catalytic properties of manganese dioxides has surged due to the attention attracted by the tremendous resource of deep-sea manganese nodules. Following the pioneering work by Weisz,[7] Aomura and his colleagues published a series of papers on the adsorptive and catalytic performance of manganese nodules.[8-12] Cabrera et al.[13] showed that the activity of manganese nodules is comparable to that of pure nickel in methanation of carbon monoxide.

Nitta et al.[12] pointed out that the composition of manganese nodules varies greatly from place to place. The composition can also be incredibly heterogeneous even in a single particle. Chukhrov et al.[14] showed that the crystallographic structure is highly diversified for todorokite, which is present as the main component in manganese nodules. These inhomogeneities impose difficulties for applications of manganese nodules as adsorbents or catalysts.

The synthesis of todorokite, with definite composition and structure, has been reported by Golden.[15] However, the thermal stability of these materials[15] seems inadequate for catalytic purpose. Studies concerning preparation of todorokites in our laboratory[16] led to the synthesis of some materials with significantly higher thermal stability as compared to previous methods. Such synthetic todorokites, featuring well-defined structures and constrained dimensionally, offer the possibility of more versatile applications in many fields. Some of these octahedral molecular sieve (OMS) materials have shown some interesting features as oxidation catalysts.[16]

Todorokite as a mineral, can be visualized as having a nominal formula of $T_2Mn_4^{2+}Mn_9^{4+}O_{24}{\cdot}9H_2O$ (T = Cu, Ni, Zn, Mg, Co). Todorokite structure is constructed

[†] Department of Chemistry.
[‡] Department of Chemical Engineering.
[§] Institute of Materials Science.
* To whom correspondence should be addressed.
[⊗] Abstract published in *Advance ACS Abstracts,* August 15, 1994.

(1) Katz, K. *Adv. Catal.* **1953**, *5*, 177.
(2) Hasegawa, S.; Yasuda; K.; Mase, T.; Kawaguchi, T. *J. Catal.* **1977**, *48*, 125.
(3) Prasad, R.; Kennedy, L. A.; Ruckenstein, E. *Catal. Rev. Sci. Eng.* **1984**, *26*, 1.
(4) Nardi, J. C. *J. Electrochem. Soc.* **1985**, *132*, 1787.
(5) Bach, S.; Pereira-Ramos, J. P.; Baffier, N.; Messina, R. *Electrochim. Acta* **1991**, *36*, 1595.
(6) Sabine, T. M.; Hewat, A. N. *J. Nucl. Mater.* **1982**, *110*, 173.
(7) Weisz, P. B. *J. Catal.* **1968**, *10*, 407.
(8) Matsuo, K.; Nitta, M.; Aomura, K. *Sekiyu Gakkai Shi* **1976**, *19*, 745.
(9) Matsuo, K.; Nitta, M.; Aomura, K. *Sekiyu Gakkai Shi* **1979**, *22*, 212.
(10) Matsuo, K.; Nitta, M.; Aomura, K. *J.* Catal. **1978**, *54*, 445.
(11) Nitta, M.; Matsuo, K.; Aomura, K. *Chem. Lett.* **1979**, 325.
(12) Nitta, M. *Appl. Catal.* **1984**, *9*, 151.
(13) Cabrera, A. L.; Maple, M. B. *Appl. Catal.* **1990**, *64*, 309.
(14) Chukhrov, F. V.; Gorshov, A. I.; Dritz, V. A. *Izv. Akad. Nauk. SSSR. Ser. Geol.* **1985**, 61.
(15) Golden, D. C.; Chen, C. C.; Dixon, J. B. *Science* **1986**, *231*, 717.
(16) Shen, Y. F.; Zerger, R. P.; Suib, S. L.; O'Young, C. L. *Science* **1993**, *260*, 511.

0897-4756/94/2806-1803$04.50/0

from triple MnO_6 octahedra sharing edges in one dimension which generates a 3 × 3 tunnel structure by vertex sharing between the chains.[17] Zeolites are composed of SiO_4 and AlO_4 tetrahedra, whereas todorokite (as well as ramsdellite, hollandite, cryptomelane, etc.) can be visualized generically as octahedral molecular sieves (OMS). This means that metal ions are octehedrally coordinated to oxygen ions. Large cations and water molecules occupy tunnel sites and stabilize the tunnel structure. The 3 × 3 OMS tunnel structure, with various doped cations, are designated hereafter as OMS-1.

Some of the framework manganese ions are in lower valency states, as Mn(II) in order to maintain electrical neutrality. The availability of such intimately coupled Mn^{4+}/Mn^{2+} sites may allow electron exchange between Mn^{4+} and Mn^{2+} or Mn^{3+} (if present) and mobility of oxygen across the surface and throughout the bulk. The ease of exchange of surface oxygen with the surrounding environment may also be enhanced.

The doping of cations (especially transition metal cations) into the OMS-1 structure further enhances the mobility of such oxygen species. Such mobile oxygen species play a dominant role during catalysis with OMS-1. In this study, temperature-programmed techniques as well as pulse techniques were used to investigate mobile oxygen species. Oxygen mobility and the activity of oxygen species in OMS-1 doped with various cations toward hydrogen, carbon monoxide, and some simple hydrocarbons were also studied.

Experimental Section

TPD and TPR. The preparation of OMS materials containing Mg, Cu, Ni, Zn, and their compositions have been described elsewhere.[16] For temperature-programmed desorption (TPD) studies, 10–20 mg of sample was loaded into the midsection of a Pyrex tubular reactor, of internal diameter 4 nm and length 400 mm, spaced with Pyrex glass wool, and placed into a tubular furnace, of internal diameter 25 mm and length 320 mm. The sample was treated from 298 to 943 K with a ramping rate of 15 K/min, under a stream of He gas, of UHP grade, and further purified with a liquid nitrogen (LN_2) trap, at 7 sccm.

Evolution of oxygen from the sample was monitored with a thermal conductivity detector (TCD) in a Varian Series 1400 GC, and signals were recorded with an HP 3396 Series (TCD) in a Varian Series 1400 GC, and signals were recorded with an HP 3396 Series II integrator, which was interfaced with an IBM 286 PC to collect data for further processing. The amount of oxygen evolved was calibrated by a standard oxygen pulse from a loop of known volume. For temperature-programmed reduction (TPR) experiments, the same procedure and precautions were observed as in TPD experiments. A 5.02% H_2 in Ar gas was used for TPR by H_2, and the water evolved was trapped with LN_2/ethanol mixture. Note that none of the TPD/TPR data (vide infra) reported here contain contributions from H_2O or CO_2. Meanwhile a 4.90% CO in He gas was used for TPR by CO, and the CO_2 formed was trapped with LN_2. Both gases were provided by Air Products and Chemicals, Allentown, PA. The TPR peak area was calibrated against the TPR of freshly calcined CuO of the same weight under the same condition with H_2/Ar and CO/He, respectively.

Pulse Reactions. Pulse reactions of OMS samples with *n*-butane and with carbon monoxide and of depleted OMS materials with oxygen were carried out in the same setup provided with a six-port two-way switching valve to introduce *n*-butane, carbon monoxide, and oxygen in a loop, of volume 63.5 μL, by a continuous stream of He gas at 30 sccm. All the products in the effluents of the *n*-butane pulse and carbon monoxide pulse were condensed with cold traps, either LN_2/ethanol or LN_2, so that the change in TCD signal is due to the change in amount of *n*-butane or carbon monoxide. The amount of OMS material used in all pulse experiments was 10 mg.

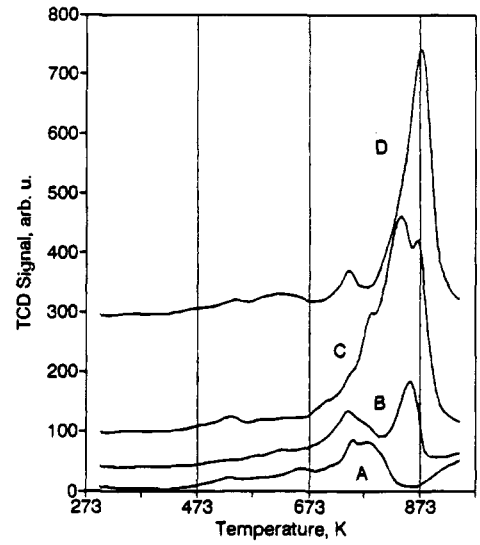

Figure 1. TPD spectra of oxygen of Metal OMS in helium: (A) Cu-OMS-1; (B) Zn-OMS-1; (C) Ni-OMS-1; (D) Mg-OMS-1.

Results

TPD. Figure 1 shows the oxygen TPD results for OMS-1 doped with Cu, Zn, Mg, and Ni, respectively. The TPD spectra of oxygen different OMS-1 materials into helium are somewhat similar in shape. Obviously, the high-temperature (HT) peak is the predominant peak for all the OMS-1 samples studied, which generally emerges in the temperature range 785–943 K. The exception is the HT peak of Cu-OMS-1 which possesses an onset temperature at 723 K. There are some low-temperature (LT) and medium-temperature (MT peaks of much lower intensity, usually merging with HT peaks, and, consequently, are difficult to separate. It is apparent that the LT peaks evolve generally below 553–563 K and could set in as low as 453 K for Cu-OMS-1. The peaks intermediate between the LT and HT peaks have to be grouped into MT Peaks. Temperatures at which they emerge can range from 563 to 785 K.

TPR. The TPR in H_2/Ar spectra of OMS-1 are shown in Figure 2, which seem to be much simpler than spectra in TPD experiments, having just two to three sharp and well-discernible peaks throughout a narrower temperature range. They can be easily designated as LT, MT, and HT peaks. The features of the TPR/H_2 spectra differ from the TPD data in that the emerging peaks diminish in intensity significantly with increasing temperature of TPR, and they shift to much lower temperatures. The Cu-OMS-1 sample is somewhat unique since it manifests two unresolved peaks in the temperature range 483–605 K, which is lower than the other M-OMS-1 samples.

The onset temperature of the LT peaks increases from Cu to Ni, to Zn, and to Mg. The onset temperature of the MT peaks generally show the same sequence. Only the Zn-OMS-1 sample definitely shows an HT peak above 713 K, and Ni-OMS-1 shows a faint tailing above 680 K. Corresponding TPR in CO/He spectra of the

(17) Post, J. E.; Bish, D. L. *Am. Mineral.* **1988**, *73*, 861.

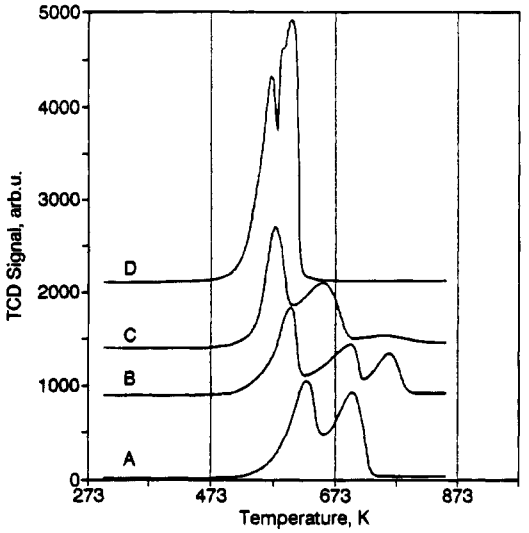

Figure 2. TPR spectra of metal OMS-1 samples in hydrogen/argon: (A) Mg-OMS-1; (B) Zn-OMS-1; (C) Ni-OMS-1; (D) Cu-OMS-1.

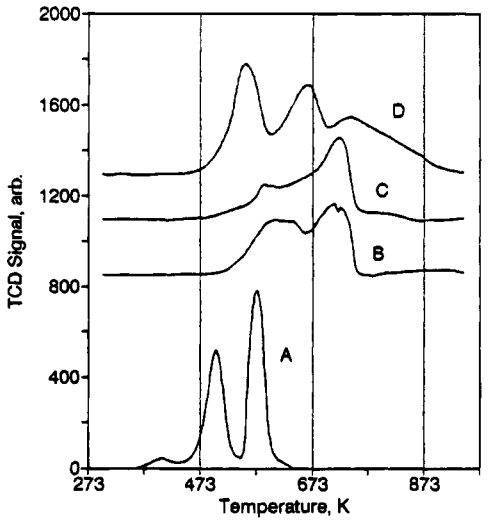

Figure 3. TPR spectra of metal OMS-1 samples in carbon monoxide/helium: (A) Cu-OMS-1; (B) Mg-OMS-1; (C) Zn-OMS-1; (D) Ni-OMS-1.

OMS-1 are shown in Figure 3. It is apparent that the TPR of Cu-OMS-1 samples in CO/He starts at even lower temperature (370 K) than in H_2/Ar. The Ni-OMS-1 shows rather similar TPR spectra in both H_2/Ar and in CO/He, although the peaks shift to lower temperature in the case of TPR in CO/He. Mg-OMS-1 and Zn-OMS-1 generally follow a similar pattern, except the peaks are poorly resolved.

Besides reactivity toward hydrogen and carbon monoxide, OMS-1 materials are demonstrated to be able to react with methane, the most inert among the paraffins. Results for TPR with methane are shown in Figure 4. Of course, much higher temperatures (at least 100 K higher) are needed to start the reaction of OMS-1 with methane. The TPR peaks are not so clean-cut. Among them, Cu-OMS-1 again shows apparently higher reactivity toward methane.

While the temperature-programmed desorption, reduction, and reaction results offer preliminary knowledge related to the distribution of oxygen species, the treatments are rather exhaustive and probably culminate in damage to the tunnel structure. Further insight into the availability of oxygen species under milder

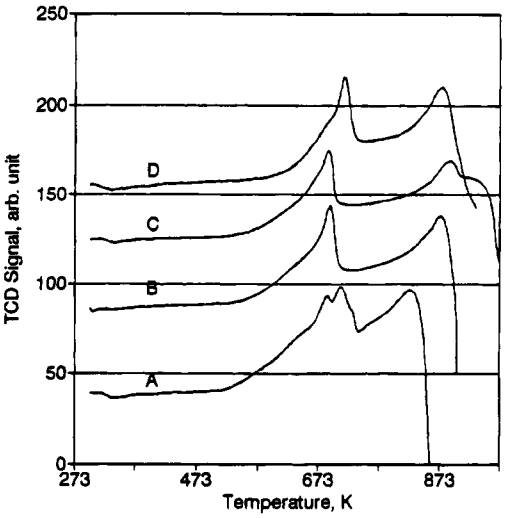

Figure 4. TPR of metal OMS-1 samples with methane in helium: (A) Cu-OMS-1; (B) Mg-OMS-1; (C) Zn-OMS-1; (D) Ni-OMS-1.

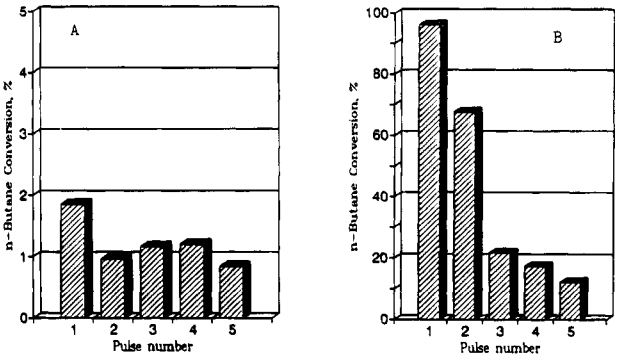

Figure 5. Pulse reaction of *n*-butane with Cu-OMS-1: (A) 423 K; (B) 573 K.

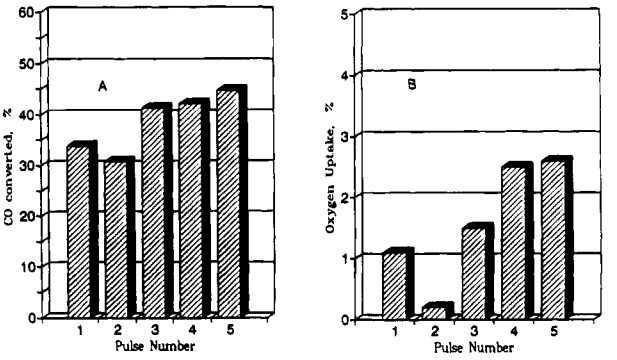

Figure 6. Pulse reaction of Cu-OMS-1 with CO/He and oxygen at 473 K: (A) pulse reaction of CO with Cu-OMS-1 at 473 K; (B) pulse reaction of Cu-OMS-1 with O_2 after reaction with CO pulses.

conditions to minimize the damage of the framework is obtained through pulse reactions. Cu-OMS-1 was used for the pulse reactions as it seems to be more catalytically active than others. The results of pulse reactions of *n*-butane with Cu-OMS-1 are depicted in Figure 5, which shows a rather high initial reactivity of Cu-OMS-1 toward *n*-butane only at 573 K. Pulse reactions carried out at 423 K show only very limited conversion of butane.

Pulse Reactions. The results of pulse reactions of Cu-OMS-1 with CO at 473 K are shown in Figure 6A. Considerable conversion of CO pulses was observed, which seems to be steady at least after five pulses, as compared with a drastic drop in *n*-butane conversion.

However, the Cu-OMS-1 depleted of oxygen atoms seems reluctant to replenish oxygen when oxygen pulses are passed at the same temperature, as shown in Figure 6B. The small amount of oxygen in the second pulse is real, the maximum experimental error is about 0.1.

Discussion

Effect of Dopant Metals. The TPD spectra of OMS-1 show some characteristic features of manganese dioxide or manganite perovskites. Iwamoto et al.[18] studied, among many oxides, the TPD of manganese dioxide, prepared by calcination of manganese salt. Seiyama et al.[19] studied the TPD of unsubstituted and substituted manganite perovskites. All these TPD spectra show predominant peaks above 923 K, with minor peaks between 523 and 673 K continuously. This suggests that such features in the TPD of these manganese-containing oxides are primarily due to the oxygen atoms bound to manganese in OMS-1.

Other cations presented either in A-sites in perovskites or in tunnel positions in todorokites, exert only a minor influence on the evolution of oxygen species during TPD. This is understandable if one takes into consideration the total number of Mn−O bonds versus the total number of T−O (T = Ni, Cu, Zn, Mg) bonds in the OMS-1 structure. The levels of metal dopants are all <5 wt %, whereas the Mn levels are usually at least 30 wt %. There is no doubt that the oxygen anions are subjected mainly to the influence of Mn ions, as in manganese dioxide, in which the Mn−O distance was reported to be 1.90 Å.[20]

Oxygen Evolution. During TPD and TPR operations, oxygen species are removed from the OMS-1 either by release into an oxygen-free gas stream or by reaction with hydrogen or carbon monoxide. These oxygen species may be adsorbed monooxygen or dioxygen as well as structural lattice oxygen. Kung[21] has suggested that there are three types of surface oxygen species evolved during TPD of metal oxides. The LT species is believed to be due to adsorbed molecular oxygen (≈423 K), at intermediate temperature adsorbed atomic oxygen is desorbed, and lattice oxygen is evolved at high temperature (≈623 K). The presence of oxygen cluster ions have been discussed in detail;[22] however, they are generally present at low levels on surfaces and will not be discussed here. Generally speaking, as the OMS-1 materials studied in this paper do not possess a large surface area (74 m^2/g for Cu-OMS-1, for example), the amounts of physisorbed or chemisorbed oxygen monolayer can be estimated to be about 0.87 mmol/g, about 4% of the total oxygen in OMS-1. Since the peak areas have been calibrated with known amounts of oxygen gas pulses for TPD and known amounts of cupric oxide for TPR in H_2 or CO, the amounts of oxygen removed corresponding to the TPD/TPR peaks can be calculated.

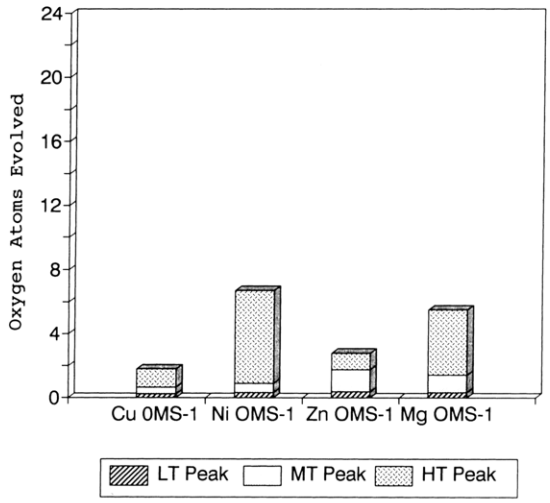

Figure 7. Distribution of oxygen species evolved per OMS-1 molecular during TPD in helium.

Distribution of Oxygen Species. According to the aforementioned chemical formulas, there are 24 structural oxygen/OMS-1 molecule; Figure 7 shows the distribution of LT, MT, and HT oxygen species, corresponding to the respective peaks, that can be released from OMS-1 into a He stream. The total oxygen evolved during TPD ranges from about two atoms (Cu-OMS-1) to seven atoms (Ni-OMS-1). Thus, we believe most of the oxygen species can be ascribed to structural oxygen bound to the lattice. As oxygen transport from the bulk to the surface is usually a rather fast process, especially in oxides with vacancies as in this case, there is no need to discern surface and bulk oxygen species.

From Figure 7, it is obvious that only rather small amounts of oxygen can be evolved into a He stream at the low and medium temperatures. The amounts of LT species (0.2−0.4 atom/molecule) and their evolving temperatures usually seem to be rarely affected by variation in the doping cation. This fact can be rationalized by assigning these amounts to chemisorbed oxygen on OMS-1. The amount of MT species ranges from 0.5 and 1.4 atoms/molecule of OMS-1. Here the effect of doping cation is observable with respect to both the evolving temperature and the amount of the MT species. From the amount of the MT oxygen species released from OMS-1, it is preferable to assign these to be due to structural oxygen.

Considerable amounts of oxygen can be released at high temperatures. The amounts of HT oxygen species (ranging from 1.1 to 6.1 atoms/molecule) released during TPD of OMS-1 greatly exceed the amount of monolayer chemisorption capacity of oxygen. These species are again likely due to structural oxygen. The effect of doping cations, although a minor one, becomes more evident when the peak positions and amounts of the HT oxygen release in TPD are compared. The ease of release of HT oxygen species, related inversely to peak temperature, bears some relationship with the heat of formation of the oxide of the doping cation. Both increase in the order Cu < Ni < Zn < Mg.

However, even at temperatures up to 943 K, a large majority of oxygen atoms remains in the sample. At least three-fourths of them are not removed by heating in an oxygen-free environment. The retention of oxygen in OMS-1 samples of Cu and Zn seems much higher than those of Ni and Mg, especially the Cu-OMS-1 sample which retains up to 90% of the oxygen.

(18) Iwamoto, M.; Yoda, Y.; Yamazoe, N.; Seiyama, T. *J. Phys. Chem.* **1978**, *82*, 2564.
(19) Seiyama, T.; Yamazoe, N.; Eguchi, K. *Ind. Eng. Chem., Prod. Res. Dev.* **1985**, *24*, 19.
(20) Rogers, D. B.; Shannon, R. D.; Sleight, A. W.; Gillson, J. L. *Inorg. Chem.* **1969**, *8*, 841.
(21) Kung, H. H. Studies in Surface Science and Catalysis, Transition Metal Oxides; Elsevier: Amsterdam, 1989; Vol. 45.
(22) Che, M.; Tench, *Adv. Catal.* **1983**, *32*, 1.
(23) Shannon, R. D.; Prewitt, C. T. *Acta Crystallogr.* **1969**, *25*, 925.
(24) Haber, J. In *Catalysis—Science and Technology*: Boudart, M., Ed.; Butterworth: London, 1984; Vol. 2.
(25) Bielanski, A.; Haber, J. In *Oxygen in Catalysis*; Dekker: New York, 1991.

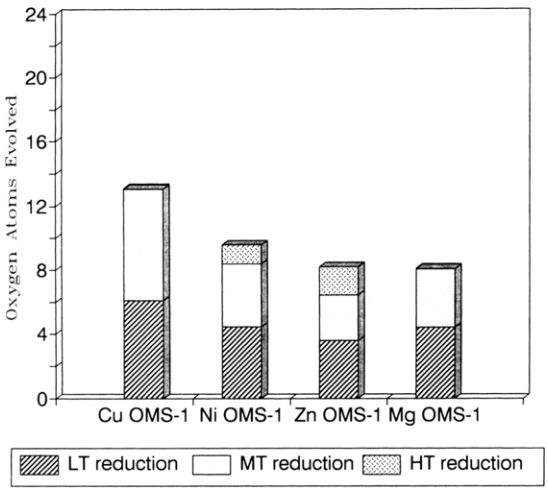

Figure 8. Distribution of oxygen species evolved per OMS-1 molecular formula during TPR in hydrogen/argon.

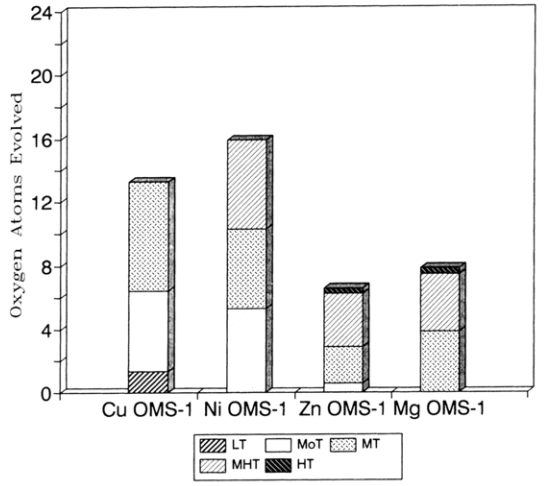

Figure 9. Distribution of oxygen species evolved per OMS-1 molecular formula during TPR in carbon monoxide/helium.

The distribution of oxygen species in the LT, MT, and HT regimes during TPR in H_2/Ar is shown in Figure 8. It is apparent that much more oxygen can be removed from the OMS-1 structure by either hydrogen or carbon monoxide. Here, the effect of doping cation is much more pronounced in TPR with hydrogen, especially in the LT and MT regimes. In the case of Cu-OMS-1, only about one-half of the structural oxygen remains after TPR with H_2/Ar. The total availability of oxygen species toward hydrogen reduction generally decreases in the order Cu > Ni > Zn > Mg, consistent with an increasing order of heat of formation of these oxides. In addition, the onset temperatures of the LT and MT peaks increase in the order Cu < Ni < Zn < Mg. Both trends are consistent with an increasing order of the heat of formation of these oxides. The same trends for a comparison of heats of formation and temperature effects for release of oxygen have been reported.[26]

The great majority of oxygen species that are active toward H_2 have roughly the same amounts of LT and MT species for individual OMS-1 materials. Cu-OMS-1 however, seems to be the most susceptible to reduction, or, in other words, it possesses more active and more available active oxygen species toward hydrogen reduction, in view of the onset temperature of reduction and the amount of LT oxygen species.

The TPR/CO spectra for most of the OMS-1 materials are somewhat more complex than the TPR/H_2 spectra. Only Cu-OMS-1 shows a clean-cut three-peak spectrum during TPR in CO/He. For other OMS-1 samples, the broad and adjoining peaks, especially for Zn-OMS-1 and Mg-OMS-1, suggest the presence of moderate-temperature (Mo-T) and medium-high-temperature (MHT) species in addition to LT, MT, and HT species. We tentatively separate these species as shown in Figure 9. Some features observed during TPR in H_2/Ar are also manifested in the TPR in CO/He. The feature of equal amounts of MoT, MT, MHT (except LT and HT) species is also observed for TPR in CO/He of each individual OMS-1 sample. For example, Ni-OMS-1 features a rather even distribution among MoT (≈555 K), MT (≈665 K), and MHT (up to 740 K) oxygen species. Moreover, there is much more availability of reactive oxygen than in TPD experiments. There are similar effects of doping cation. Besides, there is considerably higher reactivity of Cu-OMS-1 and Ni-OMS-1 than Zn-OMS-1 and Mg-OMS-1 materials. The Cu-OMS-1 and Ni-OMS-1 also possess a considerable amount of oxygen species in the lower temperature regimes (<673 K) that are much less for other M-OMS-1 materials. The depletion of oxygen by TPR in CO/He reaches two-thirds and one-half of the total oxygen in Ni-OMS-1 and Cu-OMS-1, respectively.

From Figure 7, it is observed that the amounts of LT and MT oxygen species released in TPD are 0.2-0.4 and 0.5-1.4 atom/molecule of OMS-1, respectively. Meanwhile, from Figures 8 and 9, the amounts of LT and MT oxygen species active during TPR in hydrogen are 3.6–6.1 and 2.9–7.0 atoms/molecule of OMS-1, respectively, and 1.1–6.7 and 3.8–6.7 atoms/molecule of OMS-1, respectively, for TPR in carbon monoxide. Obviously, the oxygen available during reduction is much greater than that during TPD. Thus, a question is raised as to whether the oxygen species that can be released to an oxygen-free environment are exactly the same entities as those reactive toward carbon monoxide and hydrogen.

In fact, it is quite possible that TPR with CO and H_2 lead to reduction of the T ions. In certain cases, there may be reduction to the metallic state and in others only partial reduction. The TPR results given here may be influenced by reduction of Cu and Ni, however, it is unlikely that Zn^{2+} or Mg^{2+} are reduced. We are now studying the surface properties of these materials with X-ray photoelectron spectroscopy.[27]

Nature of Oxygen Species. As yet there is no evidence from other in situ physicochemical measurements of the OMS-1 samples during TPD or TPR to enable assignment of the oxygen species. We would like to suggest that most of the oxygen that can be released at high temperature into helium streams reactive toward reductant are lattice oxygens bound to manganese. However, they can be differentiated into species of different binding strengths to manganese, and the binding strengths are liable to change under different conditions. Such species can be mutually interconverted. Tentatively, the oxygen can be discerned into three species. The α-species are weakly bound adsorbed oxygen species, which can be released in the LT region during TPD.

(26) (a) Satterfield, C. N. *Heterogeneous Catalysis in Practice*; McGraw Hill Co.: New York, 1980; pp 182–198. (b) Boreskov, G. K.; Buyanov, R. A.; Ivanov, A. A. *Kinet. Catal.* **1967**, *8*, 126.

(27) Suib, S. L.; Willis, W. S., manuscript in preparation.

It is known that there are Mn^{2+} ions present in the framework of OMS-1 for maintaining electrical neutrality due to incorporation of tunnel cations. Consequently, oxygen atoms in the framework bound to the Mn^{2+} ions have a weak interaction, as the bond distances between Mn^{2+}–O, 2.23 Å,[23] are significantly greater than the Mn^{4+}–O bond distance in OMS-1. It is suggested that these oxygen atoms, classified as β-species, are liable to be released in the MT region during TPD, as compared to those bound more strongly to Mn^{4+}, the γ-species. The amount of Mn^{2+} ions in the framework of OMS-1 samples is less than one-half of that of Mn^{4+}. Consequently, the amounts of β-species released during TPD are much less than the most abundant γ-species.

However, during TPR with hydrogen or carbon monoxide, new Mn^{2+} ions are readily formed and those γ-oxygen species now become bound to newly formed Mn^{2+} ions at lower binding strengths and turn into weakly bound β-species which are more reactive to hydrogen and carbon monoxide. Thus, the nascent β-species are formed at the expense of γ-species, resulting in a reversed population in TPR as compared to TPD. It is presumed that no new Mn^{2+} ions are formed after the removal of γ-oxygen species during TPD, possibly as a result of anion vacancies or crystallographic shear.[24] Of course, during TPR, with either hydrogen or carbon monoxide, the weakly bound adsorbed α-oxygen species, possibly in the dioxygen form, are also consumed in the LT regime.

The more facile reduction of OMS-1 in carbon monoxide than in hydrogen is of no surprise, as other systems are consistent with this idea.[25] The more pronounced effect on doping cations on TPR in hydrogen or carbon monoxide suggests a possibility that they are more mobile after the onset of reduction and migrate to a position closer to the tunnel walls. Thus they can exert more influence on the Mn–O–T bridge and affect the reactivity of oxygen atoms. Their effect can be tentatively related to their different electronegativities. Cu has the greatest electronegativity (2.0), nickel the second (1.8), succeeded by Zn (1.6), and Mg (1.2). Greater electronegativity further weakens the Mn–O bond and leads to higher reactivity toward reductants than in the low electronegativity systems. The electronegativity of an element bears a direct relationship with the heat of formation of the oxide of that element. The enhanced mobility of the doping cations may be related to the formation of anion vacancies during reduction.

Recovery of Oxygen. Although Cu-OMS-1 seems to be the most active toward TPR, pulse reactions with *n*-butane reveal that is is quite unreactive toward butane at low temperature. Even at temperatures as high as 573 K, the first butane pulse can have a nearly complete conversion, but successive pulses show a drastic drop in conversion. The amount of oxygen in the Cu-OMS-1 reactive to the five pulses of *n*-butane can be estimated to be about 3.4 atoms/molecule. This implies a limited availability of reactive oxygen species for butane oxidation.

Meanwhile, Cu-OMS-1 manifests a rather sustained efficient reactivity toward carbon monoxide pulses at 473 K. From Figure 6A, it can be estimated that the total amount of oxygen reacted with the five pulses of carbon monoxide is about 0.7 atom among the 24 oxygen atoms in the Cu-OMS-1 material. Figure 6B shows that the replenishment of oxygen by the reaction of depleted Cu-OMS-1 with oxygen pulses is only 0.03 oxygen atom. Meanwhile, the oxygen depleted during reaction with carbon monoxide pulses at 443 K amounts to only 0.06 atom/Cu-OMS-1. Remembering that Cu-OMS-1 shows considerable activity toward CO catalyzed oxidation at 393 K in the presence of air,[16] these data seem to imply that an associative mechanism of oxidation (hydrocarbon or CO and adsorbed oxygen) prevails at low reaction temperature (<450 K) versus a Mars van Krevelen mechanism (hydrocarbon or CO and lattice oxygen).

A reviewer has pointed out that it is reasonable to observe a much larger CO conversion than butane conversion in pulse reactions. This is true because every CO molecule will consume one oxygen atom, whereas every butane molecule will consume 13 oxygen atoms.

The inability to totally take up the same amount of oxygen that was lost is due to structural collapse of these materials under these TPD and TPR conditions. XRD data for treated materials suggest that they are amorphous after these treatments.

Conclusions

Several oxygen species can be discriminated in the tunnel structure of OMS-1 in view of the emerging temperature of peaks during TPD or TPR in H_2/Ar and CO/He. The predominance of oxygen species related to the HT peak in TPD suggests they are mainly under the influence of Mn ions in the framework due to their much larger content than the dopant metal (T) concentration.

The evolution of peaks is affected less significantly by the doping cations for the case of TPD of OMS-1, but remarkably influenced for the case of TPR in both H_2/Ar and CO/He with respect to both emerging temperature and population.

Cu-doped OMS-1 appears to possess more oxygen species that are especially reactive to H_2 and CO at low temperatures. In some cases, the decreased reactivity of oxygen species in OMS-1 doped with various cations seems to be related to the heat of formation of the oxides of the doping cation.

The population of oxygen species in different temperature regimes is quite different for TPD and TPR. The reversal in population of oxygen species in TPD and in TPR is explained as due to the reduction of tetravalent Mn during TPR.

It is rational to classify oxygen species emerging in TPD and TPR as pertaining to adsorbed oxygen, to oxygen bound to framework Mn^{2+}, and to oxygen bound to framework Mn^{4+}.

Butane and methane can be oxidized over OMS-1 in the absence of oxygen to different extents. Carbon monoxide can be oxidized in the absence of oxygen to a much greater extent. Replenishment of depleted oxygen into OMS-1 may be slow for regeneration of OMS materials.

Acknowledgment. We acknowledge Texaco, Inc., and the Department of Energy, Office of Basic Energy Sciences, Division of Chemical Sciences for support of this research.